# Nanoluciferase complementation-based biosensor reveals the importance of N- linked glycosylation of SARS-CoV-2 Spike for viral entry

**Taha Azad** ( tazad@ohri.ca )
Ottawa Hospital Research Institute https://orcid.org/0000-0002-9498-0657
**Ragunath Singaravelu** ( rsingaravelu@ohri.ca )
Ottawa Hospital Research Institute
**Zaid Taha**
Ottawa Hospital Research Institute
**Stephen Boulton**
Ottawa Hospital Research Institute
**Mathieu J.F. Crupi**
Ottawa Hospital Research Institute
**Nikolas T. Martin**
Ottawa Hospital Research Institute
**Taylor Jamieson**
Ottawa Hospital Research Institute
**Joanna Poutou**
Ottawa Hospital Research Institute
**Mina Ghahremani**
University of Ottawa
**Adrian Pelin**
Ottawa Hospital Research Institute
**Kazem Nouri**
Queen's University Kingston,
**Rozanne Arulanandam**
Ottawa Hospital Research Institute
**Emily E.F. Brown**
Ottawa Hospital Research Institute
**Reuben Samson**
Lunenfeld-Tenenbaum Institute
**Anne-Claude Gingras**
Lunenfeld-Tenenbaum Institute
**Peter A. Greer**

Queen's University Kingston
**Carolina S. Ilkow**
Ottawa Hospital Research Institute
**Jean-Simon Diallo**
Ottawa Hospital Research Institute
**John C. Bell** ( jbell@ohri.ca )
Ottawa Hospital Research Institute

---

**Research Article**

**Keywords:** coronavirus, bioluminescence, biosensor, viral entry, high-throughput screening, 2019-nCoV, SARS-CoV-2, COVID-19

**Posted Date:** August 14th, 2020

**DOI:** https://doi.org/10.21203/rs.3.rs-58455/v1



---

**Version of Record:** A version of this preprint was published at Molecular Therapy on August 14th, 2020. See the published version at https://doi.org/10.1016/j.ymthe.2021.02.007.

# Abstract

The ongoing COVID-19 pandemic has highlighted the` immediate need for the development of antiviral therapeutics targeting different stages of the SARS-CoV-2 lifecycle. We developed a bioluminescence-based biosensor to interrogate the interaction between the SARS-CoV-2 viral spike protein and its host entry receptor, angiotensin-converting enzyme 2 (ACE2). The biosensor assay is based on a Nanoluciferase complementation reporter, composed of two subunits, Large BiT and Small BiT, fused to the spike receptor-binding domain (RBD) of the SARS-CoV-2 S protein and ACE2 ectodomain, respectively. Using this biosensor, we uncovered a critical role for glycosylation of asparagine residues within the RBD in mediating successful binding to the cellular ACE2 receptor and subsequent virus infection. Our findings support RBD glycosylation as a therapeutic and vaccine target to blunt SARSCoV- 2 infections.


# Introduction

As of July 25, 2020, there are globally over 15.5 million confirmed SARS-CoV-2[4] infections resulting in nearly 640 thousand deaths[5] and with no signs of the pandemic ebbing in the near future, effective therapeutics and vaccines are desperately needed. Entry of the enveloped SARS-CoV-2 virus into mammalian cells is mediated by the viral Spike (S) protein that binds to the *A*ngiotensin *C*onverting *E*nzyme *2* (*ACE2*) cell receptor and initiates fusion of the viral and cell membranes. This critical role in the virus infection cycle has made the S protein the focus of therapeutic development including the identification of neutralizing antibodies[7], peptide-based S protein binders[6] and small molecule inhibitors of proteases involved in S protein maturation[3]. Like many enveloped virus surface proteins, S is heavily glycosylated and it is has been speculated that these post-translational modifications could facilitate immune evasion or perhaps play a fundamental role in the determination of virus tropism [6]. Interestingly, two N-linked glycan modifications occur within the conserved *R*eceptor *B*inding *D*omain or *RBD* of the S protein. The RBD mediates the binding of the S protein to ACE2[7, 8] and while there have been a number of documented polymorphisms in the amino acid sequence of the RBD from clinical isolates around the world[9], these two glycosylation sites are uniformly conserved. This suggested to us the possibility that glycosylation of the RBD is important for its binding to the cellular ACE2 receptor or as suggested earlier inhibits immune recognition. To test these ideas, we constructed a biosensor to rapidly assess the interactions between RBD variants and the ACE2 receptor. We took advantage of the recently developed NanoLuc Binary Technology (NanoBiT) [10, 11 12] to create a surrogate assay for virus:host cell interactions. Our biosensor provides a simple and rapid system to carry out a structure-function analysis of critical amino acids in the RBD that modulate its interaction with ACE2. We demonstrate that the two conserved N-glycan modifications in RBD are required for efficient binding to ACE2 and infection with S pseudotyped viruses.

# Results

### SARS-CoV-2 NanoBiT biosensor for detecting ACE2-RBD interactions

Several different reporter fragment complementation-based strategies have been employed to interrogate protein-protein interactions[13], including split-luciferase schemes[14-16 17]. Conventional split-luciferase bioreporters can be limited in their application due to their relatively large sizes, poor stability, and the short half-lives of their catalyzed luminescent reactions. The recently reported Nanoluciferase (or NanoLuc from *Oplophorus gracilirostris*)[18] does not possess these limitations, and a NanoLuc-based fragment complementation system has been reported [10, 11 12]. Our biosensor employs NanoLuc fragments linked to RBD and ACE2 creating a biosensor that can rapidly and sensitively serve as a surrogate for virus:host cell interactions (Fig. 1A). Using published sequences and structural homology analysis[7, 8, 19, 20], we designed a SARS-CoV-2 RBD sequence spanning residues 331 to 524 of the S protein (194 amino acids; Supplementary Fig. 1) for one component of the biosensor. For the other component we used the soluble ectodomain of ACE2 (residues 1 to 740) as this has been shown to be sufficient to interact with RBD[21]. Since RBD is the smaller protein of the two partners of interest[11], we linked the RBD with the larger fragment of the split luciferase (LgBiT) while ACE2 was fused to the small fragment (SmBiT, Figure 1B). A glycine-serine linker was inserted between ACE2 or RBD and its respective NanoBiT component[11] to enhance folding and flexibility of the fusion proteins. To facilitate the production of the interacting partners as secreted molecules, we carried out a series of codon optimization studies and tested different secretion signals. We found good production and complementation with an interleukin-12 secretion signal linked to the SmBiT-ACE2 fusion protein while an IgK secretory leader sequence worked best at the N-terminus of the RBD-LgBiT protein. Transfection of these constructs into 293T cells showed strong expression in cell lysates and secretion into supernatants, as confirmed by immunoblot analyses (Fig. 1C). We then carried out luciferase assays using either cell lysates or supernatants from 293T cells co-transfected with RBD and ACE2 NanoBiT fusion constructs in both orientations (Fig. 1D). As can be seen, SmBiT-ACE2 and either RBD-LgBiT or LgBiT-RBD (>$10^5$ RLU vs ~$10^4$ RLU in Fig. 1C) produced strong luminescent signals compared to transfection of individual components.

Supernatants from the co-transfected cells also produced strong luminescence in the assay mirroring our findings with the cell lysates (Fig. 1D). The large dynamic range of the assay makes it amenable to high-throughput screening and indeed bioluminescent signals could even be observed using an IVIS imaging system or with the naked eye (Supplementary Fig. 2B). We validated the specificity of the interactions we were detecting in two ways. First we co-transfected SmBiT-ACE2 or LgBiT-RBD with LgBiT- YAP15 or SmBiT-14-3-3, respectively. While the YAP15 and 14-3-3 constructs have been previously demonstrated to interact and rescue the NanoBiT structure[11], these proteins are not known to interact with ACE2 and RBD. As predicted, LgBiT-Yap15 and SmBiT-14-3-3 proteins did not complement SmBiT-ACE2 or LgBit-RBD respectively (Fig 1E ). Second we evaluated the impact of recombinant soluble ACE2 protein (rACE2), a SARS-CoV-2 entry inhibitor under clinical investigation as an antiviral[22], and recombinant RBD (rRBD) on the SARS-CoV-2 NanoBiT. For these experiments, we transfected 293T cells independently with either the RBD-LgBiT or SmBiT-ACE2 constructs to obtain lysates or culture supernatants containing either RBD-LgBiT or SmBiT-ACE2. In the absence of added recombinant protein, the combined lysates or

supernatants produced robust signals (Fig. 1F). However, upon pre-incubation of RBD-LgBiT with rACE2 prior to adding the SmBiT-ACE2 containing lysate, we observed dose dependent reduction in luminescent signal (Fig. 1F). Similarly, pre-incubation of SmBiT- ACE2 with recombinant RBD resulted in the loss of luminescence in the biosensor reporter assay (Fig. 1G). These results serve as proof-of-principle that our biosensor can identify molecules which disrupt the ACE2-RBD interaction. We also constructed a SARS-CoV-1 NanoBiT biosensor. Earlier work suggested that the SARS-CoV-2 RBD binds with higher affinity to ACE2 than SARS-CoV-1 RBD, potentially contributing to the virus' enhanced transmissibility[8] while others have shown that the RBDs from these two viruses have comparable affinities[7, 23]. In our hands, the SARS-CoV-1 NanoBiT produced only a modestly reduced signal relative to the SARS-CoV-2 biosensor (Fig. 1H and Supplemental Fig. 4) supporting the idea that two virus RBDs have comparable affinity for ACE2.

## The SARS-CoV-2 Biosensor is Sensitive to Neutralizing Antibodies

Monoclonal antibodies targeting RBD are under consideration as SARS-CoV-2 therapeutics[24]. We screened 13 different commercially available monoclonal SARS-CoV-2 Spike RBD antibodies with the SARS-CoV-2 biosensor (Fig. 2A). Seven of these antibodies (# 4,5,6,7,8,9,10) are reported to not only bind RBD but also neutralize infection of cells with an S pseudotyped lentivirus. Interestingly these seven monoclonal antibodies were the most effective at blocking RBD-ACE2 interactions measured with the SARS-CoV-2 biosensor. We applied the antibody collection to the SARS-CoV-1 biosensor and found that while most SARS-CoV-2 antibodies did not cross-react, antibodies #7 and 8 showed some ability to disrupt RBD-ACE2 interactions for both virus strains. Non-specific mouse IgG and monoclonal antibody #1, which binds to the S2 subdomain of the Spike protein, did not disrupt the signal generated by the SARS- CoV-2 biosensor supporting the specificity of the signals were observed. We tested our biosensors with serum from two patients recovered from SARS-CoV-2 infections at the Ottawa Hospital and pooled serum from three healthy volunteers. In these experiments we compared our SARS-CoV-2 biosensor to a widely used, commercially available ELISA kit that is designed to act as surrogate for virus neutralization. For the biosensor experiments, SARS-CoV-2 RBD-LgBiT was co-incubated with sera for 25 min, followed by the addition of SmBiT-ACE2 for an additional five minutes. At this point, substrate was added and luminescence measured. The biosensor was able to distinguish seroconverters from healthy donors as both convalescent patients' sera significantly reduce the biosensor signal (Fig. 2B- right panel). Interestingly, sera from convalescent SARS-CoV-2 patients failed to disrupt the SARS-CoV-1 RBD-ACE2 interaction (Fig. 2B- left panel), suggesting a lack of cross-reactivity in these patients' neutralizing antibody response. The signal from our biosensor compared well with the results produced by a receptor-ligand binding ELISA from GenScript (Fig. 2C). It is worth noting, however, the NanoBiT assay is a more rapid and simplified single tube reaction.

SARS-CoV-2 genome sequencing has revealed the emergence of RBD mutations in global strains. We investigated the influence of six emerging RBD mutations found in SARS-CoV-2 genome sequences worldwide on the ACE2-RBD interaction: V367F (France and Hong Kong/China), N354D (China), A435S (Finland), F342L (England), K458R and V483R (United States)[25] (Fig. 2D). The biosensor assay revealed that these SARS-CoV-2 variants displayed variable binding to ACE2 (Fig. 2E- F). Interestingly, the V367F

mutant displayed over 3-fold enhanced interaction with ACE2, while the F342L mutation decreased reporter activity 2-fold. The enhanced affinity of V367F RBD mutation to ACE2 is consistent with a recent study describing enhanced viral entry in HEK293T-ACE2/TMPRSS2 cells with lentivirus pseudotyped with V367F Spike compared to wildtype Spike[9]. Similarly, these mutations also have the potential to impact the efficacy of RBD-targeted monoclonal antibodies and vaccination strategies. We analyzed the cross-reactivity of two SARS-CoV-2 RBD- targeted monoclonal antibodies towards the different RBD variants using the biosensor assay (Fig. 2G-H). Our results demonstrated that both monoclonal antibodies tested could effectively block all the mutants' interactions with ACE2 – highlighting that monoclonal RBD antibodies can work effectively against SARS-CoV-2 strains encoding the different RBD variants. As described below, we determined that the RBD used in our biosensor, when produced from human 293T cells, is glycosylated at the two asparagine residues sites previously identified using a site-specific mass spectrometric approach. Taken together, our results suggest that, N-linked glycans are ineffective in blocking the recognition of RBD by a spectrum of neutralizing antibodies and polyclonal patient serum. This prompted us to determine if modifications at these two sites could play a role in RBD binding to ACE2.

## N-linked glycosylation of RBD is required for ACE2-RBD interaction

We found that bacterially produced recombinant SARS-CoV-2 RBD was not able to block SmBiT-ACE2's interaction with SARS-CoV-2 RBD-LgBiT (Supplementary Fig. 5A), in contrast to our results with recombinant RBD produced in mammalian cells (Fig. 1G). An important distinction with bacterial expression systems is their inability to produce mammalian-type glycosylation, suggesting a potential role for protein glycosylation in the ACE2-RBD interaction. As discussed earlier, a recent study demonstrated that the spike protein contains 22 N-linked glycosylation sites[6] including two in the RBD at asparagine residues 331 and 343. To evaluate the relevance of N- linked glycosylation of RBD on the ACE2-RBD interaction, we pre-treated RBD-LgBiT or SmBiT-ACE2 containing lysates with peptide:N-glycosidase F (PNGase F) or endoglycosidase H (Endo H), enzymes, which cleave N-linked oligosaccharides, and subsequently interrogated their ability to interact with their complementary partner using the biosensor assay. Interestingly, RBD-LgBiT's treatment with either enzyme significantly impaired its interaction with the ACE2 ectodomain, whereas treatment of SmBiT-ACE2 had no effect (Fig. 3A). We next performed the biosensor assay using RBD-LgBiT cell lysates derived from 293T cells treated with tunicamycin, an inhibitor of N-linked glycosylation in eukaryotic cells. Immunoblot analyses demonstrated that RBD-LgBiT transfected cells which were treated with tunicamycin produced RBD-LgBiT with an apparent lower molecular weight – suggesting a loss of glycosylation (Fig. 3B). Tunicamycin treatment resulted in significantly reduced biosensor activity in lysates from cells co-transfected with RBD-LgBiT and SmBiT-ACE2 (Fig. 3C, Supplemental Fig. 5B). Taken together, this data suggests that N-linked glycosylation of the SARS-CoV-2 S protein RBD is necessary for its interaction with ACE2. To more directly determine the importance of RBD glycosylation, we substituted alanine residues for aspargines at positions 331 and 343. Immunoblot analyses of the point mutations in RBD-LgBiT revealed that N331A and N343A mutations resulted in decreased molecular weights, consistent with the

two sites being functional glycosylation sites (Fig. 3D) and paralleled the changes in mobility of RBD produced from tunicamycin treated cells. We evaluated the impact of mutating these two glycosylation sites on ACE2-RBD interactions using our biosensor assay (Fig. 3D-E; Supplemental Fig. 5C-D). Both the N331A and N343A mutations significantly impacted complementation between ACE2 and RBD fusion proteins. To further validate the importance of N-linked glycosylation to SARS-CoV-2 infectivity using an orthogonal approach, we also used Endo H and PNGase F treatment on S protein pseudotyped lentiviruses. Consistent with the biosensor data (Fig. 3A-E), enzymatic removal of N-linked glycosylation abrogated the infectivity of the S pseudotyped lentivirus (Fig. 3F). We then used site-directed mutagenesis to create full-length Spike mutants (N331A and N340A) and used these to create S pseudotyped lentiviruses. Consistent with our SARS-CoV-2-NanoBiT data (Fig. 3E), both mutations produced significant decreases in S pseudotyped lentivirus infectivity (Fig. 3G, Supplemental Fig. 5E-F). Overall, these data provide the first direct evidence that SARS-CoV-2 S depends on N-linked glycosylation of RBD to mediate its interaction with the ACE2 ectodomain.

### SARS-CoV-2-NanoBiT identifies lectins as antiviral therapeutic candidates

SARS-CoV-2 S is glycosylated with oligomannose- and complex-type glycans [6]. We sought to examine the therapeutic potential of targeting these N-linked glycans by testing mannose-binding plant lectins for anti-viral effects. We screened lectins from *Canavalia ensiformis* (jack bean), *Pisum sativum* (pea), *Galanthus nivalis* (snow drop),

*Datura stramonium* (jimson weed/thorn apple), and *Lens culinaris* (lentil) for their ability to disrupt the SARS-CoV-2 RBD-ACE2 interaction using our biosensor (Fig. 3H). Our results demonstrate a diverse range of antiviral effects. While the lentil lectin displayed no significant inhibition of the interaction across the tested concentration range (8-1000 ng/mL), other lectins showed some efficacy, with the jack bean lectin (Concanavalin A or ConA) demonstrating the strongest impact. The antiviral effects for the top two lectin candidates (*Pisum sativum* and ConA) were validated for their ability to inhibit Spike pseudotyped lentivirus at 100 ng/mL (Fig. 3I). Consistent with the CoV-NanoBiT data, both lectins inhibited pseudovirion entry, with ConA showing over a 900-fold decrease while the pea lectin showed only an 8-fold decrease. ConA's antiviral effects are consistent with previous work suggesting mannose-binding lectins can inhibit SARS- CoV infection [26]. Collectively, our work suggests targeting the glycosylation of Spike represents a viable therapeutic target that warrants further investigation.

## Discussion

Previous studies using split-luciferase reporters have examined viral protein interactions[27, 28], however we believe the data presented here is the first report of a NanoLuc complementation reporter-based assay to probe viral entry. We have validated the system's ability to successfully test potential therapeutics, including monoclonal antibodies and receptor decoys. The biosensor also enabled the evaluation of emerging RBD mutations on SARS-COV-2 infectivity and monoclonal antibody efficacy. This represents a valuable application as we begin to identify the novel emerging SARS-CoV-2 spike mutants in the global

population. Our observation that monoclonal RBD antibodies have conserved efficacy against various RBD variants suggests that vaccines capable of inducing a strong neutralizing antibody response against SARS-COV-2 RBD should display strong cross-reactive efficacy in the global population. Although it has been speculated that glycan clusters on the Spike protein could impede immune recognition or antibody activity, our biosensor data suggests that for the Spike RBD of SARS-CoV-2 this may not be the primary role of glycosylation.

Indeed, given the strong conservation of these glycosylation sites in clinical isolates around the world we believe that appropriate glycosylation at N331 and N343 could provide a conserved target for vaccine development.

We believe that our data provides the first direct evidence demonstrating that N-linked glycosylation of SARS-CoV-2 RBD is an important mediator of ACE2 binding. We then utilized plant lectins to target this post-translational modification and inhibit the ACE2- RBD interaction and demonstrated its potential as an antiviral using a pseudovirion system. A recent study demonstrated that it was viable to engineer a banana lectin to inhibit influenza A virus infection in mice while minimizing mitogenic effects associated with lectins [29]. The most potent antiviral lectin identified in this study, ConA, may similarly act as a lead candidate to enable the development of a SARS-CoV-2 spike glycan-targeted lectin. Alternatively, our finding that glycosylation is essential for RBD binding to ACE2 suggests that it may be possible to use specific glycosylation inhibitors as an antiviral approach to blunt SARS-CoV-2 infections especially if given acutely in a locoregional fashion. For example, iminosugars that disrupt appropriate processing of N-linked glycan groups have been shown to act as broad-spectrum antivirals against viruses which dependent on one N-linked glycan on a glycoprotein for infectivity [30].

SARS-CoV-2-NanoBiT represents a versatile and rapid tool for the identification of novel inhibitors and molecular determinants of coronavirus infection. It can be easily adapted for use in high-throughput screening of drug libraries or phage display libraries. Our work further highlights the untapped potential of the NanoLuc complementation- based reporter strategy in identifying antiviral drugs targeting other host-virus interactions which will undoubtedly be critical to our global response against future pandemics.

# Materials And Methods

*2.1 Plasmid construction*

Inserts outlined in Supplementary Table 1 were ordered from GenScript. Biosensor subunits were cloned into the BamHI/NotI sites of pcDNA3.1 to generate mammalian expression constructs.

*2.2 Cell culture*

293T (ATCC® CRL-3216), HEK293 (ATCC® CRL-1573), and HEK293-ACE2 cells were cultured in Dulbecco's modified Eagle's medium (Sigma) containing 10% FBS, and 1% penicillin/streptomycin (Invitrogen). HEK293-ACE2 cells were previously described [31].

*2.3 In vitro NanoLuc assay*

293T cells ($3\times10^5$ cells) were plated in 12 well plates in triplicate 24 h before transfection. Five hundred nanograms of the biosensor constructs were transfected using PolyJet transfection reagent (SignaGen Laboratories). After 48 h, supernatant or cells lysates were collected. Cells were lysed using passive lysis buffer (Promega).

NanoLuc luciferase assays were performed using one of two substrates: furimazine (FMZ; Nano-Glo Cell Reagent, Promega) or native coelenterazine (CTZ; 3.33 mM final concentration; Nanolight Technologies – Prolume Ltd., Pinetop, AZ, USA). Synergy Microplate Reader (BioTek, Winooski, VT, USA) was used to measure luminescence. Results are presented as RLU (Relative Luminescence Unit) normalized to control. The data presented are the mean of three independent experiments.

*2.4 Bioluminescence imaging*

Lysates or supernatants from 293T cells transfected with the biosensor construct were imaged in a 96 well plate. Nano-Glo Cell Reagent was added to the lysate in a 96 well plate as per the manufacturer's protocols for the NanoLuc luciferase assay kit (Promega). Plates were imaged with the IVIS 200 Series (Xenogen Corp.). Data acquisition and analysis was performed using the Living Image v2.5 procedure in the Igor Pro 4.09 software.

*2.5 Structure analysis*

Protein sequence alignments were performed using Clustal Omega[32]. X-ray crystal structures for the RBDs of SARS-CoV and SARS-CoV-2 in complex with ACE2 were obtained from the Protein Data Bank (PDB IDs: 2AJF and 6M0J, respectively) and visualized with PyMOL (Version 2.0 Schrödinger, LLC.)[19, 20]. The RBD alignment and RMSD calculations were also performed in PyMOL.

*2.6 Biosensor-based neutralization assay*

For neutralization assay with monoclonal antibodies and patient sera, 5 mg RBD-LgBiT containing cell lysates were incubated at 37°C for 25 min with candidate antibodies or serum. Then 50 mg of SmBiT-ACE2-transfected cell lysate was added, and incubated for an additional five minutes at room temperature. Subsequently, luciferase assay was performed. The following monoclonal RBD antibodies were tested in the biosensor- based neutralization assay: 1A9 (GeneTex; GTX632604); 2414 (ActiveMotif 91349), 1414 (ActiveMotif 91361), 273074 (Abcam ab273074); 40592 (Sino Biological 40592- MM57); 9ACA (GenScript 5B7D7), 11D11F2 (GenScript), 10G6H5 (Genscript), HC2001 (GenScript), and L00847 (Genscript Biotech).

*2.7 Pseudovirus assay*

SARS-CoV-2 spike pseudotyped lentivirus were produced as previously described using plasmids kindly provided by Dr. Jesse Bloom (Fred Hutchinson Cancer Research Center, Seattle, WA) [31]. For glycosite

mutants, HDm-IDTSpike-fixK was mutated using QuikChange SDM kit (Stratagene) using the primers listed in Supplementary Table 1, as per manufacturer's protocols. Briefly, HEK293 cells were co-transfected with HDM- IDTSpike-fixK, pHAGE-CMV-Luc2-IRES-ZsGreen-W, and pSPAX2. 48 hours post-transfection, cell supernatants containing virus were collected and treated with either PNGase F or EndoH for 1 hours. HEK293-ACE2 cells were subsequently transduced and transduction efficiency was assessed by luciferase assay using the Bright-Glo Luciferase Assay system (Promega) or fluorescence microscopy (EVOS Cell Imaging System, Thermo Fisher). Where indicated, lentivirus titers were measured using Lenti-X GoStix Plus (Takara) as per manufacturer's protocols. For lectin inhibition assays, Spike pseudotyped lentivirus was co-incubated with lectins for 1 hour, and then virus/lectin mixture was applied to HEK293-ACE2 cells as described above.

2.8 *Surrogate SARS-CoV-2 neutralization assay*

Receptor-ligand binding ELISA was performed as per manufacturer's protocols (GenScript L00847).

*2.9 Statistical analysis*

All graphs and statistical analyses were generated using Excel or GraphPad Prism v.8. Means of two groups were compared using two-tailed unpaired Student's t-test. Means of more than two groups were compared by one-way ANOVA with Dunnett's or Tukey's multiple comparisons correction. Alpha levels for all tests were 0.05, with a 95% confidence interval. Error was calculated as the standard deviation (SD). Measurements were taken from distinct samples. For all analyses, *P<0.05, **P<0.01, ***P<0.001,****P<0.0001; n.s. = not significant. Data was reproduced by two different operators.

*2.10 Other materials*

PNGaseF (P0704S) and Endo H (P0702S) was purchased from NEB. RBD (230-30162- 100) and ACE2 (00707-01-05B) recombinant protein was purchased from RayBiotech respectively. Lectins used in this study were purchased from Sigma-Aldrich (L2766, L5380, L8275, L7647) or Millipore Sigma (L1277).

# Declarations


## Acknowledgments

LgBiT-YAP15 and 14-3-3-SmBiT plasmids were gifts from Dr. Yang (Queen's University, Canada). Schematic pictures were designed by Dr. Mina Ghahremani (Designs that Cell). TA acknowledges the Banting Fellowship for funding support. RS is supported by post-doctoral funding from CIHR. TA, RS, NTM, MJF, and JP are recipients of funding support from MITACS Accelerate. JCB, JSD and CSI are supported by grants from the CCSRI, CIHR and TFFRI. ZT acknowledges NSERC for funding support in the form of a graduate scholarship Thanks to This Week in Virology for inspiration, specifically Dr. Vincent Racaniello.

### Authors contribution

Taha Azad: Conceptualization, Methodology, Investigation, Formal Analysis, Visualisation. Writing – Original Draft, Reviewing & Editing. Ragunath Singaravelu: Investigation, Writing – Original Draft, Reviewing & Editing. Zaid Taha: Investigation,Writing – Original Draft, Reviewing & Editing. Nikolas T. Martin – Investigation. Stephen Boulton: Formal Analysis, Writing: Reviewing & Editing. Mathieu Crupi: Investigation, Writing – Reviewing & Editing. Joanna Poutou: Investigation. Mina Ghahremani: Conceptualization, Investigation, Illustration. Kazem Nouri: Conceptualization. Rozanne Arulanandam: Investigation, Writing – Reviewing & Editing. Peter A. Greer: Conceptualization, Reviewing and Editing. Carolina S. Ilkow: Writing – Reviewing and Editing. Jean-Simon Diallo: Writing – Reviewing and Editing. John C. Bell – Supervision, Conceptualization, Writing – Original Draft, Review & Editing, Funding Acquisition, Program Administration.

### Declaration of competing interest

The authors have no competing interests.

# References


1. Li, W. et al. Receptor and viral determinants of SARS-coronavirus adaptation to human ACE2. *The EMBO Journal* **24**, 1634-1643 (2005).
2. Walls, A.C. et al. Structure, Function, and Antigenicity of the SARS-CoV-2 Spike Glycoprotein. *Cell* (2020).
3. Hoffmann, M. et al. SARS-CoV-2 Cell Entry Depends on ACE2 and TMPRSS2 and Is Blocked by a Clinically Proven Protease Inhibitor. *Cell* (2020).
4. Li, Q. et al. Early Transmission Dynamics in Wuhan, China, of Novel Coronavirus–Infected Pneumonia. *New England Journal of Medicine* (2020).
5. WHO (2020).
6. Watanabe, Y., Allen, J.D., Wrapp, D., McLellan, J.S. & Crispin, M. Site-specific glycan analysis of the SARS-CoV-2 spike. *Science*, eabb9983 (2020).
7. Sun, C. et al. SARS-CoV-2 and SARS-CoV Spike-RBD Structure and Receptor Binding Comparison and Potential Implications on Neutralizing Antibody and Vaccine Development. *bioRxiv*, 2020.2002.2016.951723 (2020).
8. Tai, W. et al. Characterization of the receptor-binding domain (RBD) of 2019 novel coronavirus: implication for development of RBD protein as a viral attachment inhibitor and vaccine. *Cellular & Molecular Immunology* (2020).
9. Ozono, S. et al. Naturally mutated spike proteins of SARS-CoV-2 variants show differential levels of cell entry. *bioRxiv*, 2020.2006.2015.151779 (2020).

10. Dixon, A.S. et al. NanoLuc Complementation Reporter Optimized for Accurate Measurement of Protein Interactions in Cells. *ACS Chemical Biology* **11**, 400-408 (2016).
11. Kazem Nouri et al. A kinome-wide screen using a NanoLuc LATS luminescent biosensor identifies ALK as a novel regulator of the Hippo pathway in tumorigenesis and immune evasion. *The FASEB Journal* **33**, 12487-12499 (2019).
12. Nouri, K. et al. Identification of Celastrol as a Novel YAP-TEAD Inhibitor for Cancer Therapy by High Throughput Screening with Ultrasensitive YAP/TAZ-TEAD Biosensors. *Cancers* **11** (2019).
13. Azad, T., Tashakor, A. & Hosseinkhani, S. Split-luciferase complementary assay: applications, recent developments, and future perspectives. *Analytical and Bioanalytical Chemistry* **406**, 5541-5560 (2014).
14. Remy, I. & Michnick, S.W. A highly sensitive protein-protein interaction assay based on Gaussia luciferase. *Nature Methods* **3**, 977-979 (2006).
15. Paulmurugan, R. & Gambhir, S.S. Monitoring Protein–Protein Interactions Using Split Synthetic Renilla Luciferase Protein-Fragment-Assisted Complementation. *Analytical Chemistry* **75**, 1584-1589 (2003).
16. Azad, T. et al. A LATS biosensor screen identifies VEGFR as a regulator of the Hippo pathway in angiogenesis. *Nature Communications* **9**, 1061 (2018).
17. Ataei, F., Torkzadeh-Mahani, M. & Hosseinkhani, S. A novel luminescent biosensor for rapid monitoring of IP3 by split-luciferase complementary assay. *Biosensors and Bioelectronics* **41**, 642-648 (2013).
18. Hall, M.P. et al. Engineered Luciferase Reporter from a Deep Sea Shrimp Utilizing a Novel Imidazopyrazinone Substrate. *ACS Chemical Biology* **7**, 1848-1857 (2012).
19. Lan, J. et al. Crystal structure of the 2019-nCoV spike receptor-binding domain bound with the ACE2 receptor. *bioRxiv*, 2020.2002.2019.956235 (2020).
20. Li, F., Li, W., Farzan, M. & Harrison, S.C. Structure of SARS Coronavirus Spike Receptor- Binding Domain Complexed with Receptor. *Science* **309**, 1864-1868 (2005).
21. Wong, S.K., Li, W., Moore, M.J., Choe, H. & Farzan, M. A 193-Amino Acid Fragment of the SARS Coronavirus S Protein Efficiently Binds Angiotensin-converting Enzyme 2. *Journal of Biological Chemistry* **279**, 3197-3201 (2004).
22. Monteil, V. et al. Inhibition of SARS-CoV-2 Infections in Engineered Human Tissues Using Clinical-Grade Soluble Human ACE2. *Cell* **181**, 905-913.e907 (2020).
23. Wrapp, D. et al. Cryo-EM structure of the 2019-nCoV spike in the prefusion conformation. *Science* **367**, 1260-1263 (2020).
24. Wang, C. et al. A human monoclonal antibody blocking SARS-CoV-2 infection. *Nature Communications* **11**, 2251 (2020).
25. Ou, J. et al. Emergence of RBD mutations in circulating SARS-CoV-2 strains enhancing the structural stability and human ACE2 receptor affinity of the spike protein. *bioRxiv*, 2020.2003.2015.991844

(2020).
26. Keyaerts, E. et al. Plant lectins are potent inhibitors of coronaviruses by interfering with two targets in the viral replication cycle. *Antiviral Research* **75**, 179-187 (2007).
27. Wei, X.-F. et al. Identification of Compounds Targeting Hepatitis B Virus Core Protein Dimerization through a Split Luciferase Complementation Assay. *Antimicrobial Agents and Chemotherapy* **62**, e01302-01318 (2018).
28. Deng, Q. et al. Application of a split luciferase complementation assay for the detection of viral protein–protein interactions. *Journal of Virological Methods* **176**, 108-111 (2011).
29. Covés-Datson, E.M. et al. A molecularly engineered antiviral banana lectin inhibits fusion and is efficacious against influenza virus infection in vivo. *Proceedings of the National Academy of Sciences* **117**, 2122-2132 (2020).
30. Miller, J.L., Tyrrell, B.E. & Zitzmann, N. in Dengue and Zika: Control and Antiviral Treatment Strategies. (eds. R. Hilgenfeld & S.G. Vasudevan) 277-301 (Springer Singapore, Singapore; 2018).
31. Crawford, K.H.D. et al. Protocol and Reagents for Pseudotyping Lentiviral Particles with SARS-CoV-2 Spike Protein for Neutralization Assays. *Viruses* **12** (2020).
32. Sievers, F. et al. Fast, scalable generation of high-quality protein multiple sequence alignments using Clustal Omega. *Molecular Systems Biology* **7**, 539 (2011).

# Figures

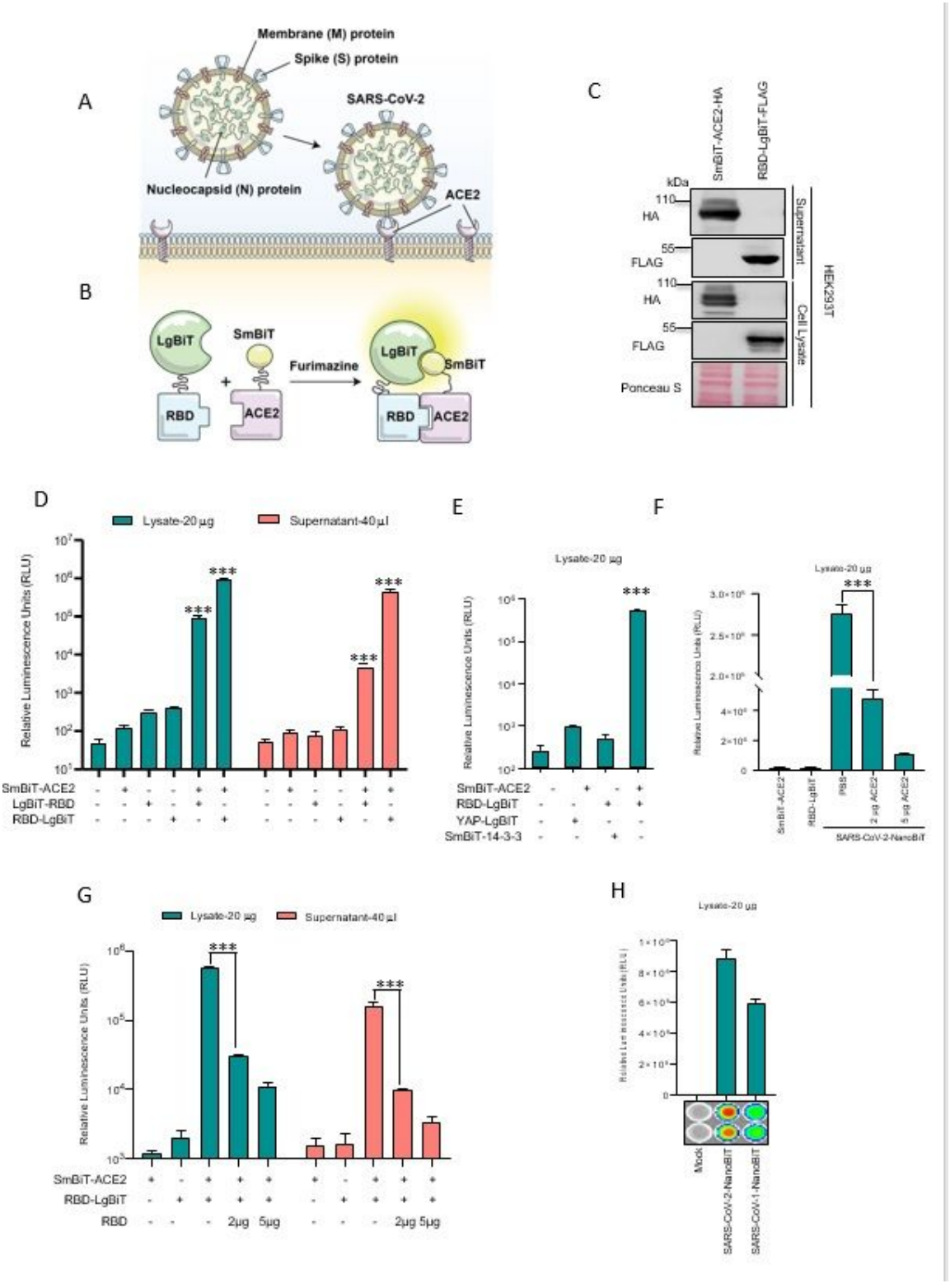


## Figure 1

Establishment of a NanoLuc complementation reporter-based biosensor for measuring ACE2 interaction with the SARS-CoV-2 Spike RBD. (A) SARS-CoV- 2 uses ACE2 as a viral entry receptor (B) Schematic depicting mechanism of action for the biosensor. (C-D) 293T cell were transfected with codon-optimized ACE2 and RBD constructs. 48 hours post-transfection, cell lysates and supernatants were harvested. 10 □g of protein or 10 □l of supernatant were resolved by SDS-PAGE. (C) Immunoblot analysis of HA-tagged

SmBiT-ACE2 and FLAG-tagged RBD-LgBiT expression. (D) Luminescence was quantified by luciferase assay using FMZ as substrate. (n=3, mean±SD; one-way ANOVA, *** $p < 0.005$ relative to RBD-LgBiT alone, Dunnett's correction for multiple comparisons). Lysates and supernatants were analyzed independently.(E) LgBiT-YAP-15 and SmBiT-14-3-3 were co-transfected with SmBiT-ACE2 and RBD- LgBiT, respectively, to demonstrate the specificity of the biosensor (n=3, mean±SD; one-way ANOVA, *** $p < 0.005$ relative to Mock, Dunnett's correction for multiple comparisons). (F) Recombinant ACE2 purified from 293T cells was incubated for 15 minutes with cell lysate containing RBD-LgBiT at room temperature. Equal amounts of lysates containing SmBiT-ACE2 were added (total 20 □g) and incubated for 5 minutes. Luciferase assay was performed using CTZ as substrate. (n=3, mean±SD; one-way ANOVA, *** $p < 0.005$, Tukey's correction for multiple comparisons.) (G) Recombinant RBD purified from 293T cells was incubated for 15 minutes with cell lysate or supernatant containing SmBiT-ACE2 at room temperature. Equal amounts of lysates or supernatants containing RBD-LgBiT were added and incubated for 5 minutes. Luciferase assay was performed using CTZ as substrate. (n=3, mean±SD; one-way ANOVA, *** $p < 0.005$, Tukey's correction for multiple comparisons.) (H) Biosensor assay was performed on lysates of 293T cells co-transfected with SmBiT-ACE2 and either SARS-CoV or SARS-CoV-2 RBD-LgBiT constructs, respectively. IVIS imaging of bioluminescence is shown below.

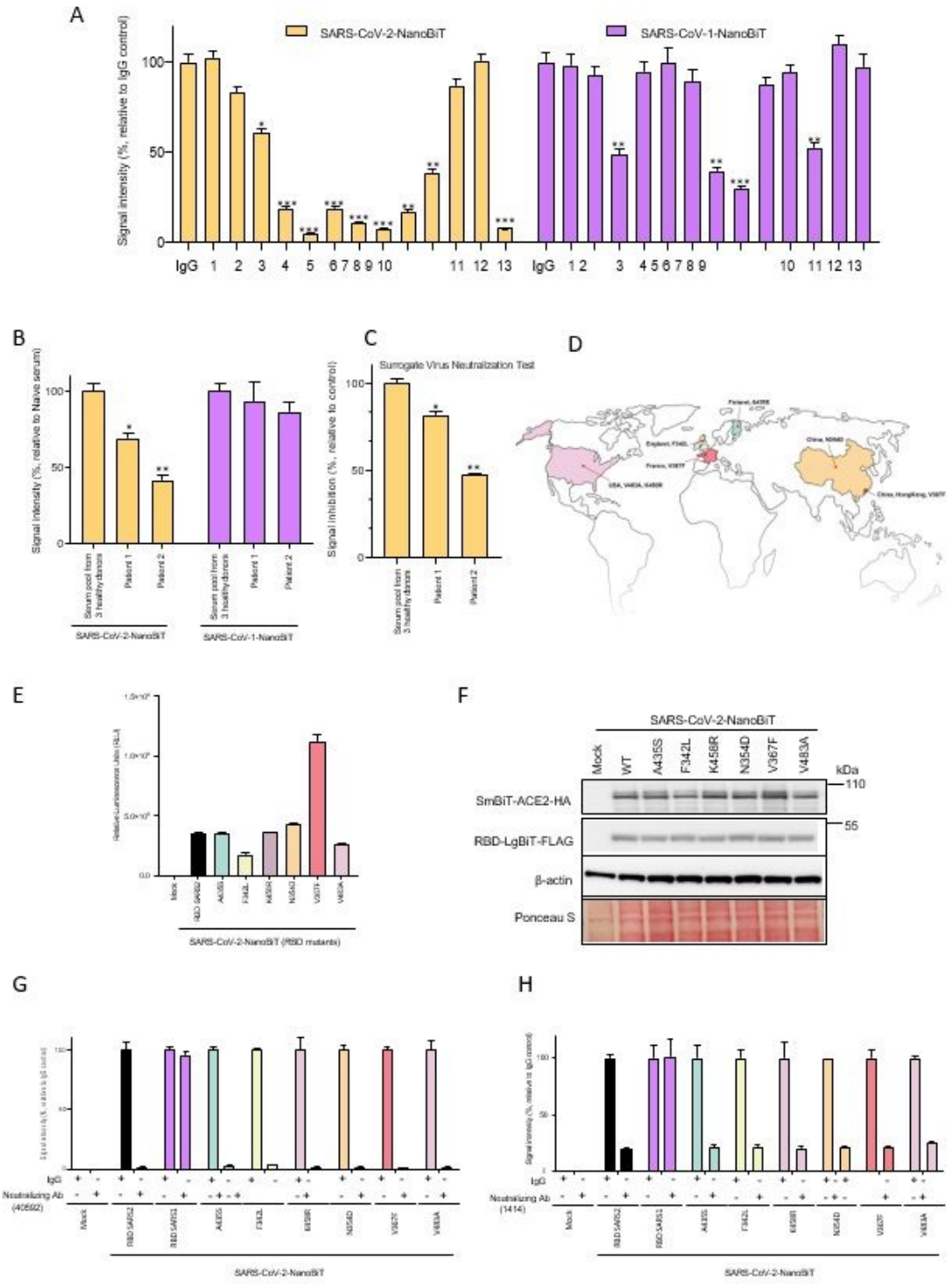


## Figure 2

SARS-CoV-2-NanoBiT enables facile detection of SARS-CoV-2 seroconversion (A) SARS-CoV-2 (left) or SARS-CoV (right) BS assays were performed with an array of anti-RBD monoclonal antibodies or control IgG. Numbers 1 to 13 refers to the following antibodies: 1: 1A9, 2: 2414, 3: 273074, 4: 1414, 5: 40592, 6: 9A9C9, 7: 5B7D7, 8: 11D5D3, 9: 6D11F2, 10: 10G6H5, 11: HC2001, 12: 13010759, 13: L00847 (B) SARS-CoV-2 BS (left) or SARS-CoV BS (right) assays were performed with serum pooled from 3 healthy donors

or two recovered SARS-CoV-2 patients for 25 minutes. Luciferase assay was performed 5 min after SmBiT-ACE2 addition. (C) SARS- CoV-2 RBD-HRP was incubated for 15 minutes with serum pool from 3 healthy donors or recovered patients from SARS-CoV2 for 25 min. Then, samples were added to a plate coated with ACE2 for 15 min. After washing, TMB solution was added and the amount of RBD-HRP binding was evaluated by measuring OD at 450 nm. (D) Geographic distribution of the SARS-CoV-2 strains with the indicated RBD mutations. (E) BS assays were performed on cells co-transfected with the indicated RBD-mutant- LgBiT constructs and SmBiT-ACE2 constructs. Also in (F) immunoblot analysis were performed to confirm the proper expression of the constructs. (G-H) Cell lysates transfected with different RBD-LgBiT mutants were incubated for 25 minutes with anti- RBD monoclonal antibodies 40592 in (G) and 1414 in (H). Luciferase assays were performed 5 minutes after SmBiT-ACE2 addition.

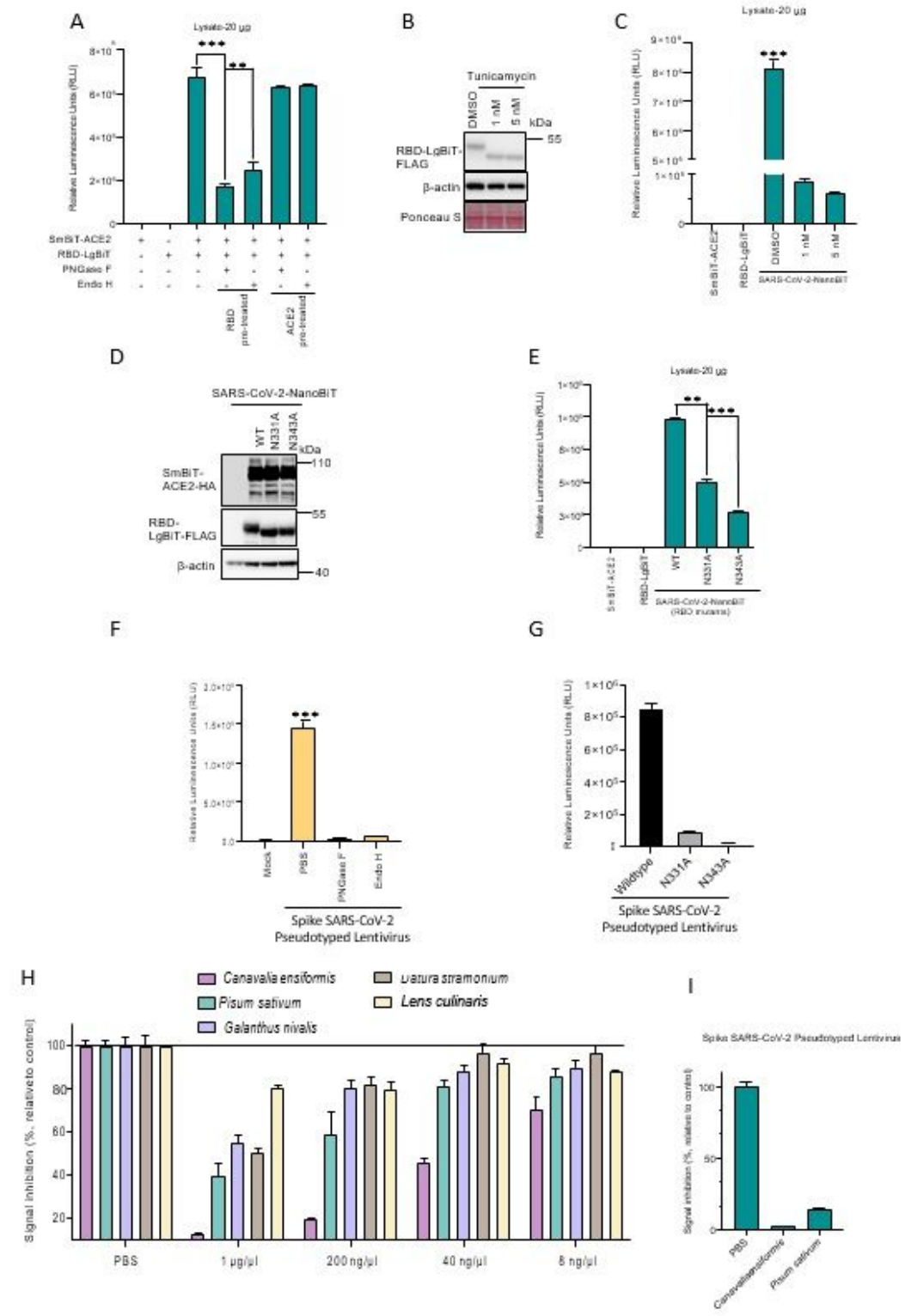


## Figure 3

N-linked glycosylation of SARS-CoV-2 Spike RBD is critical to its interaction with ACE2. (A) 293T cells transfected with either SmBiT-ACE2 or RBD- LgBiT were harvested. 10 ug of lysates were pre-treated for 1 hour at 370C with endoglycosidase H, PNGase F, or untreated, as indicated. Lysates were subsequently mixed and incubated for 15 minutes at room temperature, then assessed by luciferase assay using CTZ as a substrate (n=3, mean±SD; one-way ANOVA, *** $p < 0.005$, Tukey's correction for multiple

comparisons). (B) 293T cells were transfected with RBD-LgBiT and 24 hrs after transfection were treated with tunicamycin for 16 hrs. Lysates were prepared and analyzed by immunoblotting. (C) RBD-LgBiT cell lysates from (B) were incubated at room with cell lysates from SmBiT-ACE2 transfected cells. After 15 minutes, the BS assay was performed. (D) immunoblot analysis and (E) BS assay were performed on cells co-transfected with the indicated RBD-glycosylation site mutants of the LgBiT-RBD constructs and SmBiT-ACE2 constructs. (F) SARS-CoV-2 S pseudotyped lentivirus encoding ZsGreen and luciferase reporters was incubated with PBS, PNGase F, or Endo H for 1 hour, and then used to infect HEK293-ACE2 cells. 48 hours post-transduction, cells were evaluated for measuring luciferase activity. (G) SARS-CoV-2 S mutant pseudotyped lentiviruses infectivity assay as in (F). (H) Plant lectins were screened for ability to disrupt CoV-NanoBiT. Cell lysates transfected with RBD-LgBiT were incubated for 1 hr with different lectins from shown species. Luciferase assays were performed 5 minutes after SmBiT-ACE2 addition. (I) Plant lectins from Canavalia ensiformis (jack bean) and Pisum sativum (pea) were evaluated for inhibitory effects against SARS-CoV-2 Spike pseuotyped lentivirus infection in HEK293-ACE2 cells.

## Supplementary Files

This is a list of supplementary files associated with this preprint. Click to download.

- SupplementaryTable1.pdf
- SupplementaryFigure1.jpg
- SupplementaryFigure2.jpg
- SupplementaryFigure3.jpg
- SupplementaryFigure4.jpg
- SupplementaryFigure5.jpg